2001

Laser-Derived Particle Size Data from CRP-3, Victoria Land Basin, Antarctica: Implications for Sequence and Seismic Stratigraphy

Christopher R. Fielding
University of Nebraska-Lincoln, cfielding2@unl.edu

G. B. Dunbar
James Cook University

S. M. Bryce
James Cook University

Terra Antartica
2001, **8**(3), 255-262

Laser-Derived Particle Size Data from CRP-3, Victoria Land Basin, Antarctica: Implications for Sequence and Seismic Stratigraphy

C.R. FIELDING[1*], G.B. DUNBAR[2+] & S.M. BRYCE[2§]

[1]Department of Earth Sciences, University of Queensland, Qld 4072 - Australia
[2]School of Earth Sciences, James Cook University, Townsville, Qld 4811 - Australia
[+]Present address: Antarctic Research Centre, Victorial University of Wellington, PO Box 600, Wellington - New Zealand
[§]Present address: Australian Geological Survey Organisation, GPO Box 378, Canberra, ACT 2601 - Australia

Received 17 November 2000; *accepted in revised form* 31 October 2001

Abstract - Seven hundred and nineteen samples from throughout the Cainozoic section in CRP-3 were analysed by a Malvern Mastersizer laser particle analyser, in order to derive a stratigraphic distribution of grain-size parameters downhole. Entropy analysis of these data (using the method of Woolfe & Michibayashi, 1995) allowed recognition of four groups of samples, each group characterised by a distinctive grain-size distribution. Group 1, which shows a multi-modal distribution, corresponds to mudrocks, interbedded mudrock/sandstone facies, muddy sandstones and diamictites. Group 2, with a sand-grade mode but showing wide dispersion of particle size, corresponds to muddy sandstones, a few cleaner sandstones and some conglomerates. Group 3 and Group 4 are also sand-dominated, with better grain-size sorting, and correspond to clean, well-washed sandstones of varying mean grain-size (medium and fine modes, respectively). The downhole disappearance of Group 1, and dominance of Groups 3 and 4 reflect a concomitant change from mudrock- and diamictite-rich lithology to a section dominated by clean, well-washed sandstones with minor conglomerates. Progressive downhole increases in percentage sand and principal mode also reflect these changes. Significant shifts in grain-size parameters and entropy group membership were noted across sequence boundaries and seismic reflectors, as recognised in other studies.

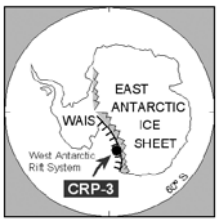

INTRODUCTION

Coring of CRP-3, the final well of the Cape Roberts Project, completed a stratigraphic transect through the western Victoria Land Basin, Antarctica. The well was drilled in October/November 1999 some 12 km offshore from Cape Roberts in McMurdo Sound (Cape Roberts Science Team, 2000 Fig. 1.1). This paper reports on laser-derived granulometric analyses performed on samples spaced approximately 1 m apart throughout the CRP-3 core. The data set is designed to address issues of stratigraphic relevance in the CRP-3 succession, and to be used in conjunction with similarly-derived data from CRP-1, -2/2A and CIROS-1 (Woolfe et al., 1998, 2000; Fielding et al., 1997, respectively), with close-spaced data from parts of CRP-2/2A and -3 (Naish et al., 2001, this volume), and with sieve/SediGraph-derived data from those cores (De Santis & Barrett 1998; Barrett & Anderson, 2000; Barrett, 1989, respectively). The principal trends and other changes evident downcore will be highlighted, interpreted, and their implications discussed in the context of the seismic and sequence stratigraphic framework for the well (Cape Roberts Science Team, 2000; Fielding et al., this volume; Henrys et al., this volume). Further, comparison will be drawn between the data set presented herein and that derived from the interval 0-150 metres below sea floor (mbsf) in CRP-3 (Naish et al., this volume). The latter data set was acquired using the same apparatus but different operating parameters, and the comparison offers some insights into the reproducibility of granulometric data measured by the laser-diffraction method.

METHODS

Particle size was determined on 719 samples (1-cm^3) at ~1-m intervals between 5.08 and 788.93-mbsf. Samples judged to be too consolidated for complete disaggregation within this interval were not analysed. All analyses were performed using a Malvern Instruments Mastersizer-X laser particle size analyzer in the Environmental Sedimentology Laboratory at James Cook University (*e.g.*, Woolfe et al., 1998).

Samples were prepared for analysis using a combination of physical and chemical treatments. First, samples were disaggregated by gently crushing between wooden blocks and a representative sub-sample (typically ~1-g) placed into a small (60-ml) beaker. Samples were then covered with 10% HNO_3 to remove carbonate and organic matter, and left to

**Corresponding author* (chrisf@earth.uq.edu.au)

stand for at least 24 hours. Additional 10% HNO_3 was then added if necessary, until effervescence ceased. Each sample was washed twice to remove reaction products and suspended in tap water. This suspension was sonicated for 5 minutes then sieved at 1000-µm to remove coarse material before being added to the Malvern sample chamber for analysis. Samples were analysed using the 1000-mm focal length lens giving a measurement range of 1.8 to 2000-µm. Previous experience has shown that material finer than the minimum size of the lens can create artefacts in the size distribution. In particular, a "false" mode is apparent at 7-µm and in some cases a secondary false mode is also created at 30-µm when a significant amount of material in the sample is finer than the minimum measurable size (Fig. 1A). However, the predominantly sandy nature of CRP-3 sediments renders this effect minor and largely confined to the upper 150-m of the core. We also note that artificial modes do not affect determination of percent sand, a key parameter of our analysis (Fig. 1B), nor do they affect our ability to compare relative differences between samples measured using the same lens configuration.

An internal JCU standard material was run prior to each batch of samples, to ensure that the instrument was operating correctly and to provide a check on the consistency of results. The reproducibility of standard measurements is shown in figure 1C. In addition, duplicate analyses were carried out on 35 core samples. The reproducibility, as determined by the difference in percentage of sand between duplicate analyses, was 6.6%. Some of this scatter can be attributed to sample inhomogeneity due to the very small sample size (1g) used for each analysis.

Subsequent to the completion of our analyses, the top 150-m of CRP 3 was resampled at 0.5 m spacing for spectral analysis (Naish et al., this volume). These samples lie between those used in this study and were analysed using the method outlined in Naish et al. (this volume). This method differs from that presented here in several ways. First, the use of a 300-mm focal length lens gives a dynamic range of 0.5 – 600-µm rather than 1.8-2000 µm. This choice of lens results in loss of some coarse sand data, although there are substantial gains in resolution and a reduction in artefacts in silt-sized material compared to the 1.8-2000-µm lens. Second, the samples were more completely mechanically disaggregated prior to sonification in an attempt to improve the efficiency of the disaggregation process. The reproducibility of sand content using this method is typically better than 2 %. Comparisons between sand % in the two laser-derived data sets, and sieve/SediGraph-derived sand percentages are presented in figure 2.

Although overall trends in % sand are similar between our data and those of Naish et al. (this volume), there are also important differences. Most

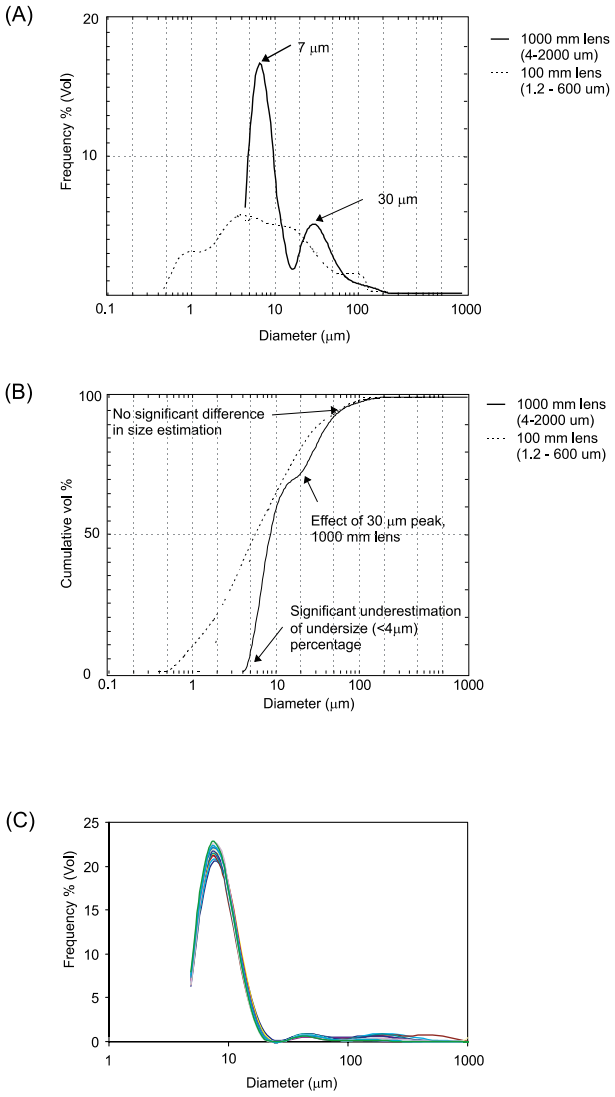

Fig. 1 - a) Comparison of frequency curves for the same sediment sample analysed using 1000 and 300 mm focal length lenses giving measurement ranges of 1.8-2000 and 0.5 – 600 um respectively. Note the artificial modes created at 7 and 30 µm when a significant proportion of the sediment is finer than the minimum range of the lens (modified after Orpin, 1999). b) cumulative undersize percent curves for the same data, showing modal artefacts do not affect sizes >50 um (modified after Orpin, 1999). c) reproducibility of an internal JCU size standard during analysis of our samples.

notable is the significantly lower % sand estimate given by the 0.5-600-µm range lens. There are several potential causes for this discrepancy. First, the measurement range of this lens only extends to 600-µm and experience suggests that material >450-µm is significantly underestimated. Typically, however, the difference in % sand is ~20% and binocular examination of the samples does not support the presence of this amount of sand in this size range. Second, incomplete disaggregation of our samples may result in artificially high percentages of sand. This is also manifest in the "spiky" nature of our record compared to that of Naish et al., (this volume). We investigated the reproducibility of the sand spike at

52.90-mbsf by reanalysing samples from 51.84, 52.90, 53.79 and 55.82 mbsf using the method of Naish et al., (2000). These results do not show an elevated sand percentage at 52.90-mbsf and are consistent with the overall trend apparent in the data of Naish et al. (this volume). Binocular microscope examination of these samples also supports the presence of relatively muddy sediment through this interval. Finally, comparison with sieve/SediGraph data of Barrett (this volume) also suggests a disaggregation problem with our data.

Systematic differences between laser and traditional methods of determining size-frequency distributions have been well documented (*e.g.* Konert & Vandenberghe, 1997; Molinaroli, et al., 2000; Hayton et al., 2001). Typically these differences are related to the varying response of each technique to deviations in grain shape from spherical (although density and other physical properties may also be important) and are most prominent in clay-sized or micaceous material. Where these effects are minor, laser and sieve/SediGraph data usually compare well (*e.g.* Hayton et al., 2001; G. Dunbar, unpublished data). In summary, although our data show clear evidence of incomplete disaggregation, most notably in mud-rich samples, overall trends between the two data sets are similar, (with the exception of a number of sand "spikes"), and therefore useful for characterising down-core changes in lithology.

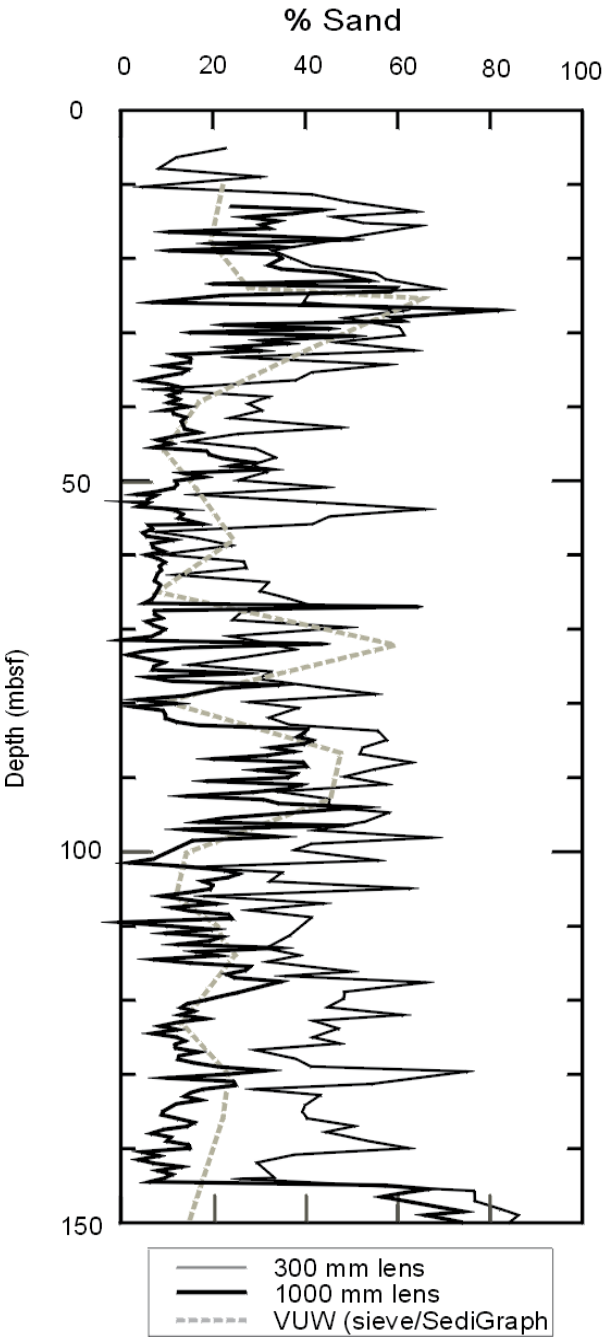

Fig. 2 - Comparison of percent sand (<1000 μm) estimates derived from analyses performed on 300 and 1000 mm focal length lenses with measurement ranges of 0.5 – 600 and 1.8-2000 μm respectively. Note that because different lenses have different size class limits, "sand" is considered to be material coarser than 56 μm and 60 μm for the 300 and 1000 mm lenses, respectively.

RESULTS

Three hundred and sixty samples were grouped using "entropy" analysis (Woolfe & Michibayashi, 1995). Software limitations precluded analysis of the entire set of 719 samples. Instead, we have included every second sample (~2-m spacing) in this analysis. Entropy analysis aims to find the optimal classification of samples into groups so that the similarity of samples within a group is maximised and the similarity between groups is minimised (Woolfe et al., 1998). This is expressed quantitatively by dividing the between-group similarity (or more correctly, inequality) for a particular grouping with the total inequality (the "Rs" value: Fig. 3). The closer the Rs

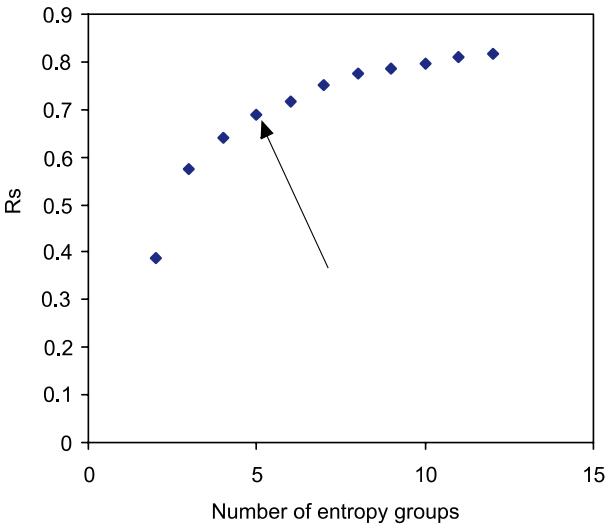

Fig. 3 - Plot of Rs value *vs.* number of Entropy groups for CRP-3 samples. The optimum number of groups occurs at N=4 (arrowed).

value is to unity, the more data can be "explained" by the grouping (Woolfe et al., 1998).

Our data were clustered into four groups following the rationale of Woolfe et al. (1998). Using this procedure, the optimum number of groups is considered to be the point at which the Rs value increases at a significantly lower rate with an increasing number of groups (in this case, four: Fig. 3). The characteristic grain-size distribution of the four groups is shown in figure 4, and the stratigraphic distribution of samples in each group is shown in figure 5.

Before considering the stratigraphic distribution of the grain-size groups, it is important to address whether there is a relationship between each group and a corresponding facies type or types. Clearly, if a strong correlation exists between each entropy group and a facies or group of related facies, then the analysis can be used more effectively to interpret stratigraphic patterns. Entropy Group 1 (Fig. 4) shows a multi-modal grain-size distribution: even given the artefact effect at the fine end of the spectrum described above, this group clearly corresponds to a clay-silt-sand mixture. Comparison between granulometric data and the core logs for CRP-3 (Cape Roberts Science Team, 2000, and see Table 1) indicates that Group 1 corresponds to mudrocks (Facies 1), interbedded mudrocks and fine-grained sandstones (Facies 2), some muddy sandstones (Facies 3) and diamictites (Facies 6, 7). Group 2 is more strongly unimodal across the spectrum of particle size measured (again allowing for the 7 μm artefact), with a dominance of sand, but shows a wide dispersion about the mode and is fine-(positively) skewed (Fig. 4). Comparison with core logs and Table 1 indicates that it corresponds principally to muddy sandstones (Facies 3), some clean sandstones (Facies 4 & 5), and many conglomerates (Facies 9 & 10). Entropy Group 3 is also unimodal with the mode in medium sand, but shows less dispersion and a more or less symmetrical distribution across the mode (Fig. 4). It displays a strong relationship with the clean sandstones of Facies 4 and 5, with minor conglomerates (Facies 9 & 10) also falling into this class (Tab. 1). Group 4 is similar to Group 3 in all aspects except that its mode lies in the fine sand range: it also correlates strongly with the clean sandstones of Facies 4 and 5 (Tab. 1). Although there is no simple relationship between Entropy Groups and facies, the stratigraphic distribution of the four groups can nonetheless be used to detect major stratigraphic changes in the facies assemblage (particularly the balance between mudrocks/diamictites (which generally occur in close association throughout the CRP cores), muddy sandstones, and clean/well-sorted sandstones.

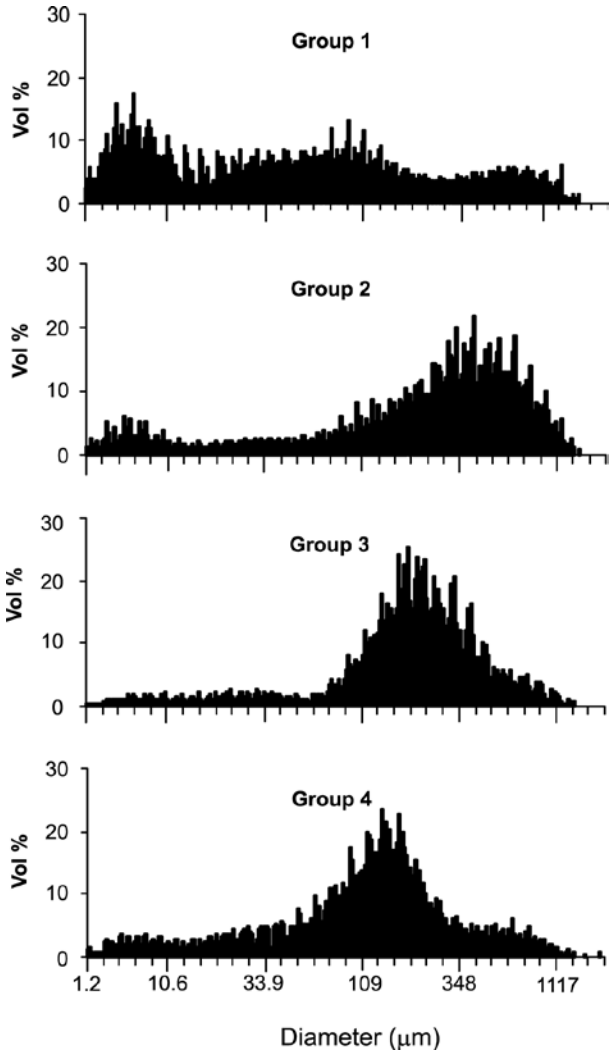

Fig. 4 - Particle size distributions of the four entropy groups used in this study. Note that modes at 7 and 30 µm are artifacts of the analysis (see "Methods" section for elaboration and Figs. 1a,b).

The downhole distribution of samples that fall into the four Entropy Groups is shown in figure 5, together with the percentage sand and principal mode of all samples (the full data set at 1 m spacing). Clear and coincident trends are evident in each of these three parameters. Furthermore, abrupt changes in these parameters occur across many if not most of the sequence boundaries recognised (Cape Roberts Science Team, 2000; Fielding et al., this volume). The clearest expression of downhole change in facies is given by the progressive increase in percentage sand, and in the principal mode, from top to bottom of the core. Concomitant changes in the distribution of Entropy Group members mirror these changes, and provide further insight into the causes of the percentage sand and principal mode trends.

Entropy Group 1 dominates the uppermost 150-m of the core (almost totally), reflecting the greater variety of lithofacies in that part of the core, and the abundance of Facies 1, 2 (mudrocks and interbedded mudrock/sandstone), 6 and 7 (diamictites). This interval corresponds also to Sequences 1-3, identified by Fielding et al. (this volume) as unusually thick and lithologically diverse, cyclical sequences that

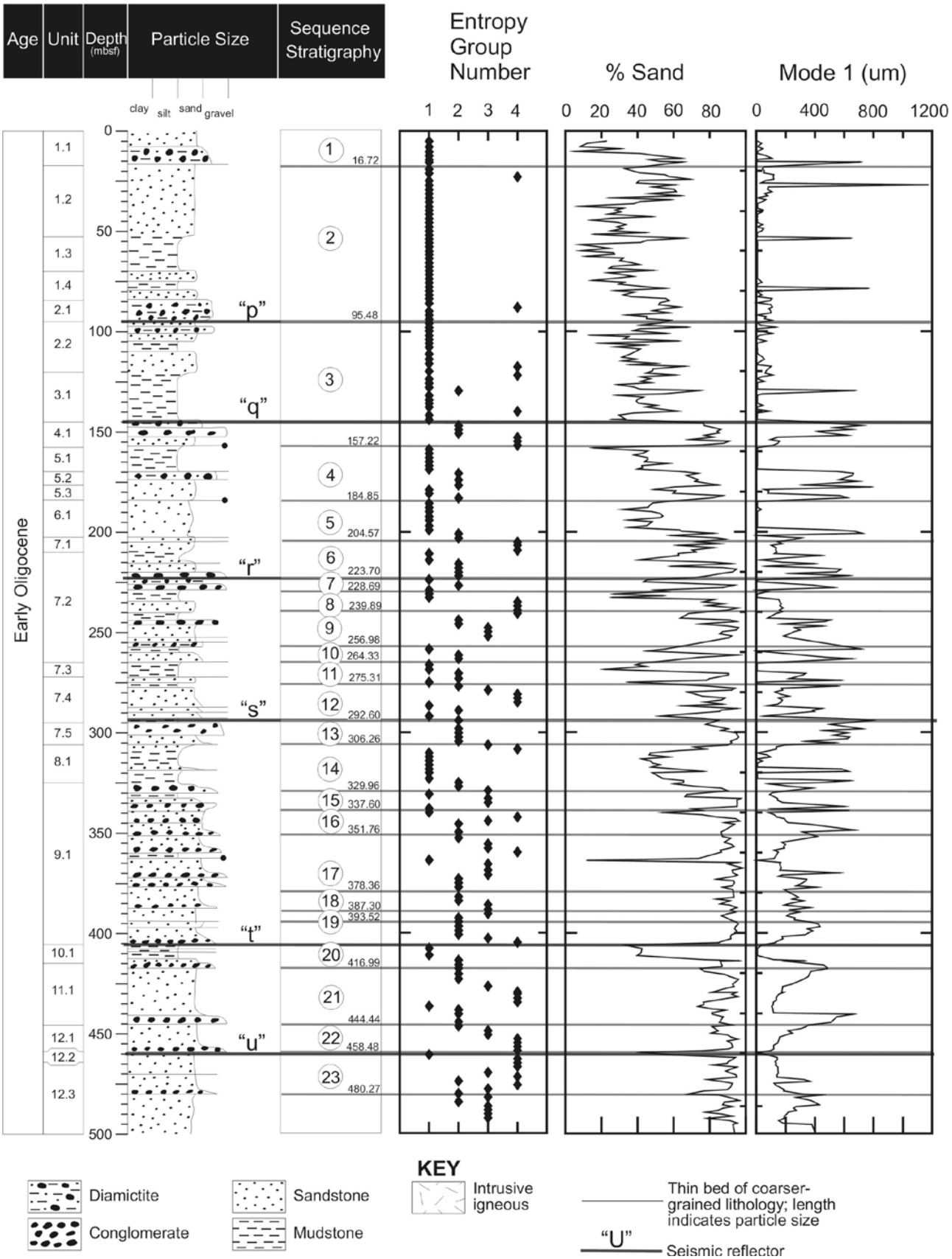

Fig. 5 - Downhole variability in entropy groups, percent sand and primary mode (gravel free) for CRP-3. Lithology and sequences boundaries are from Naish et al., (this volume). Locations of seismic reflectors are from Henrys et al. (this volume).

Tab. 1 - List of lithofacies recognised in CRP-3, and their downhole distribution.

Facies	***Lithology***	***Interpretation***	***Distribution in CRP-3***
1	Mudstone	Settling from suspension in offshore water depths	Common down to 329.96 mbsf, rare below this depth except between 762-782 mbsf
2	Interstratified sandstone/mudstone	Low-energy tractional flows and fallout from suspension	As for Facies 1.
3	Poorly sorted, muddy sandstone	High-energy deposits of ?density flows	Abundant above 378.36 mbsf and within 580-789.77 mbsf
4	Well-sorted, clean, fine-grained, stratified sandstone	Deposits of dilute, tractional flows in shoreface water depths	Uncommon between 378.36-580 mbsf, no occurrences elsewhere
5	Well-sorted, clean, fine- to medium-grained sandstone	Deposits of dilute tractional flows in shallow marine waters	Common between 378.36-580 mbsf, less common through remainder of hole
6	Stratified diamictite	Subglacial or ice-contact proglacial marine deposition	Uncommon at intervals above 378.36 mbsf
7	Massive diamictite	Subglacial or ice-contact proglacial marine deposition	Uncommon at intervals above 378.36 mbsf
8	Rhythmically interstratified sandstone and siltstone	Deposition from turbid overflow plumes associated with glacier snout efflux	Rare above 378.36 mbsf
9	Clast-supported conglomerate	Deposition from a variety of processes in shallow marine waters	Common throughout the hole
10	Matrix-supported conglomerate	Deposition from a variety of processes in shallow marine waters	Common throughout the hole

incorporate significant mudrock and diamictite intervals in addition to sandstone lithofacies. Entropy Group 1 is abundantly represented, though not as dominant, from 150 to *c*. 340-mbsf, is then rare down to 460 mbsf, and virtually absent below that depth (Fig. 5). This gradual decline in Entropy Group 1 membership corresponds to a concomitant downhole decrease in the occurrence of mudrocks, interbedded mudrock/sandstone and diamictites. The only exception to this pattern is an interval from 762 to 782 mbsf, which also contains several Group 1 members.

Entropy Group 2 is absent from the uppermost 130 m of the core, but is then abundantly represented down to 590 mbsf and rare below that depth apart from a cluster of samples within conglomerate-dominated strata between 770 and 795 mbsf (Fig. 5). Although clearly not representative of any particular lithofacies, the strong representation of Entropy Group 2 in the upper half of CRP-3 reflects the abundance of muddy sandstones (Facies 3) over that interval. The interval 770-795 mbsf also shows an abundance of Facies 3 muddy sandstones, although many of the Entropy Group 2 members in this interval may reflect conglomerates. The pattern is complicated by the presence of conglomerates elsewhere throughout the succession.

Entropy Group 3 is unrepresented above *c*.-250-mbsf, but common to abundant below that depth. This interval corresponds to that in which the clean, well-sorted sandstones of Facies 4 and 5 are most abundant in the core. The first appearance of Entropy Group 3 members downward in the core also corresponds with the change to sand-dominated lithology as shown by trends in both percentage sand and principal mode plots (Fig. 5). Entropy Group 4 is scattered to abundant throughout the core down to *c*. 600-mbsf, but then is dominant down to *c*. 765-mbsf. This pattern is interpreted to reflect the occurrence of predominantly fine-grained clean sandstones throughout the hole, but particularly concentrated in the lower 200-m of the Cainozoic succession. An antithetic relationship between Entropy Group 3 and 4 membership is evident over this interval, suggesting some genetic link between the two groups, as has already been established above.

RELATIONSHIPS WITH SEQUENCE AND SEISMIC STRATIGRAPHY

A number of reflectors have been recognised from seismic reflection data within the area of the Cape Roberts Project drillholes. Several of these occur within the succession penetrated by CRP-3 (Cape Roberts Science Team, 2000), and most also correspond to sequence boundaries or to some other notable lithological change (Fielding et al., this volume). Nearly every seismic reflector noted by Cape Roberts Science Team (2000), and modified by Henrys et al. (this volume) is recorded in some way by the grain-size data presented herein (Fig. 5). In many cases the reflector corresponds to a baseline shift in either or both of percentage sand and principal mode, while in others it matches a “spike” in one or

other of those parameters (but see Methods, regarding the reliability of such spikes).

Most of the sequence boundaries recognised in CRP-3 correspond to changes in Entropy Group membership, and nearly all correspond to shifts in percentage sand and principal mode, although variation patterns are too complicated to allow these parameters to be used to independently identify sequence boundaries (Fig. 5).

DISCUSSION AND CONCLUSIONS

The particle size data and statistical parameters derived from those data presented herein are consistent with the interpretation of geological history presented in Cape Roberts Science Team (2000) and Fielding et al. (this volume). The overwhelming impression gained from CRP-3 is of a succession that includes mudrocks and diamictites only in the uppermost 150 m, and which passes downward into a sandstone-dominated succession with increasing conglomerates to the base of the Cainozoic succession. The Entropy Groups, percentage sand and principal mode plots all show this change graphically. The transition to a succession lacking in diamictites has been interpreted to reflect a period of time when extensive ice cover was lacking in this part of Antarctica (Cape Roberts Science Team, 2000; Fielding et al., this volume), and hence the role of glaciers in controlling sediment distribution was minimal. The attendant decline in mudrock abundance downhole has been interpreted to reflect a change in accommodation.

The basal part of the Cainozoic section in CRP-3 is interpreted to record mainly subaerial environments of deposition, during the initial formation of the Victoria Land Basin rift. The section is sand and gravel-dominated, and samples from this interval are members of Entropy Groups 2-4. The fine-grained interval from 782-762 mbsf, in which Entropy Groups 1 and 4 are dominant, reflects an abrupt drowning of the depositional surface, and is interpreted by Fielding et al. (this volume) to record the acceleration of tectonic subsidence as the rift began to grow. The overlying 150 m of section is dominated by sandstones with minor conglomerates (Entropy Group 4), reflecting sediment accumulation in mainly shallow marine environments, in conditions of coarse sediment oversupply. Between 600 and 460 mbsf, Entropy Groups 2 and 3 dominate, with lesser Group 4, corresponding to a further sandstone-prone interval. Above 460 mbsf, all four Entropy Groups are well-represented, with first Group 3 and then Group 4 dying out and Group 1 becoming dominant upward: these changes mirror the progressive upward change to more heterolithic, mudstone- and diamictite-rich lithology that is interpreted to record the first influence from glacier activity in the area of the drillsites. The CRP-3 section, therefore, records the initial formation of the western Victoria Land Basin rift, and the grain-size parameters documented herein reflect a combination of tectonic processes and an emerging glacial influence through time towards the top of the section.

ACKNOWLEDGEMENTS - We are proud to acknowledge the superb effort of the Cape Roberts Project drillsite team in executing CRP-3. We also acknowledge the logistical support offered by the New Zealand and US Antarctic Programmes, without which none of this would have been possible. All scientists and support staff involved in the Cape Roberts Project are thanked for their help, advice, and vigorous scientific debate which have together made the experience such a rewarding one for us. Jaap van der Meer and an anonymous individual are thanked for their reviews of the submitted manuscript. CRF was supported by two out-of-cycle Large Grants from the Australian Research Council.

REFERENCES

Barrett P.J., 1989. Sediment texture. In: Barrett, P.J. (ed.), Antarctic Cenozoic history from the CIROS-1 borehole, McMurdo Sound, *DSIR Bulletin*, **245**, 49-58.

Barrett P.J., 2001. Grain-size analysis and preliminary interpretation of samples from the CRP-3 drillhole, Victoria Land Basin, Antarctica. This volume.

Barrett P.J. & Anderson J., 2000. Sieve and Sedigraph-derived grain-size parameters from CRP-2/2A, McMurdo sound, Antarctica. *Terra Antartica*, **7**, 373-378.

Cape Roberts Science Team, 2000. Studies from the Cape Roberts Project, Ross Sea, Antarctica: Initial Report on CRP-3. *Terra Antartica*, **7**, 1-209.

De Santis L. & Barrett P.J., 1998. Grain size analysis of samples from CRP-1. *Terra Antartica*, **5**, 375-382.

Fielding C.R., Woolfe K.J., Purdon R.G., Lavelle M. & Howe J.A., 1997. Sedimentological and Stratigraphical Re-Evaluation of the CIROS-1 Core, McMurdo Sound, Antarctica. *Terra Antartica*, **4**, 149-160.

Fielding C.R., Naish T.R., Woolfe K.J. & Lavelle M.A. 2000. Facies analysis and sequence stratigraphy of CRP-2/2A, McMurdo Sound, Antarctica. *Terra Antartica*, **7**, 323-338.

Fielding C.R., Naish T.R. & Woolfe K.J., 2001. Facies architecture of the CRP-3 drillhole, Victoria Land Basin, Antarctica. This volume.

Hayton S., Nelson C.S., Ricketts B.D., Cooke S. & Wedd M.W., 2001. Effect of mica on particle-size analyses using the laser diffraction technique. Journal of Sedimentary Research (A), **71**, 507-509.

Henrys S.A., Bücker C.J., Niessen F. & Bartek L.R., 2001. Correlation of Seismic Reflectors with Drillhole CRP-3, Victoria Land Basin, Antarctica.This volume

Konert M., Vandenberghe J., 1997. Comparison of laser grain size analysis with pipette and sieve analysis: a solution for the underestimation of the clay fraction. Sedimentology, **44**, 523-535.

Molinaroli E., De Falco G., Rabitti S., Asunta Portaro R., 2000. Stream-scanning laser system, electric sensing counter and settling grain size analysis: a comparison using reference materials and marine sediments. Sedimentary Geology, **130**, 269–281.

Naish T.R., Woolfe K.J., Barrett P.J., Wilson G.S., Atkins C., Bohaty S.M., Bucker C.J., Claps M., Davey F.J., Dunbar G.B., Dunn A.G., Fielding C.R., Florindo F., Hannah M.J., Harwood D.M., Henrys S.A., Krissek L.A., Lavelle M., van der Meer J., McIntosh W.C., Niessen F., Passchier S., Powell R.D., Roberts A.P., Sagnotti L., Scherer R.P., Strong C.P., Talarico F., Verosub K.L., Villa G., Watkins D.K., Webb P-N. & Wonik T., 2001. Orbitally induced oscillations in the East Antarctic ice sheet at the Oligocene/Miocene boundary. *Nature* **413**, 719-723.

Naish T.R., Barrett P.J., Dunbar G.B., Woolfe K.J., Dunn A.G., Henrys S.A., Claps M., Powell R.D. & Fielding C.R., 2001. Sedimentary cyclicity in CRP drillcore, Victoria Land Basin, Antarctica. This volume.

Orpin A.R., 1999. Sediment transport, partitioning, and unmixing relationships in the mixed terrigenous-carbonate system of the Great Barrier Reef, Burdekin shelf sector, Australia. Unpublished Ph.D. thesis. James Cook University.

Woolfe K.J. & Michibayashi K., 1995. "Basic" entropy grouping of laser-derived grain-size data: an example from the Great Barrier Reef. *Computers & Geosciences,* **21**, 447-462.

Woolfe K.J., Fielding C.R., Howe J.A., Lavelle M.A. & Lally J.H., 1998. Laser-derived, particle size characteristics of CRP-1. *Terra Antartica*, **5**, 383-391.

Woolfe K.J., Stewart L.K., Fielding C.R. & Lavelle M.A., 2000. Laser-derived, particle size data from CRP-2/2A: implications for sequence and seismic stratigraphy. *Terra Antartica*, **7**, 369-372.